International Journal of Emerging Engineering Research and Technology
Volume 7, Issue 3, 2019, PP 9-27
ISSN 2349-4395 (Print) & ISSN 2349-4409 (Online)

A Study on Misaligned Modulated Apertures in Confocal Scanning Laser Microscope (CSLM)

A.M. Hamed[1] and Tarek A. Al- Saeed[2]

[1]*Physics Department, Faculty of Science, Ain Shams University, 11566 Cairo, Egypt.*
[2]*Biomedical Department, Faculty of Engineering, Helwan University, Cairo, Egypt.*

***Corresponding Author:** A.M. Hamed, Physics Department, Faculty of Science, Ain Shams University, 11566 Cairo, Egypt. Email amhamed73@hotmail.com*

ABSTRACT

In this paper, we consider misaligned linear and quadratic apertures in the optical system of the CSLM. Tilting and lateral shift of the 2nd aperture is considered while the 1st objective is assumed aligned. The Point Spread Function (PSF), in both cases of linear and quadratic misaligned apertures, is computed the Result Point Spread Function (RPSF) for the CSLM is computed from the product of the PSF corresponding to each objective lens. A comparison of the PSF in case of misaligned apertures with that of aligned apertures is given. The input bone marrow image, using the misaligned apertures, is processed considering the CSLM. The output images are computed from the modulus square of the convolution product of the input image and the RPSF computed for the aligned and the misaligned apertures. An empirical formula for the Coherent Transfer Function (CTF) corresponding to the misaligned linear and quadratic apertures is obtained. A comparison of the CTF in both cases of aligned and misaligned objectives is given.In addition, the contrast of the reconstructed images is computed in both cases of aligned and misaligned apertures and compared with the contrast of the original image.

Keywords: *Misaligned Linear And Quadratic Apertures, Image Processing, The Resultant Point Spread Function In CSLM.*

INTRODUCTION

The famous work on the PSF is made by Sheppard et. al. [1-12] using annular and Gaussian apertures. Improvement of axial resolution in confocal microscopy using annular pupil is investigated in [9].Practical limits of resolution in confocal and nonlinear microscopy is presented in [11]. The effect of numerical aperture on interference fringe spacing is shown in [13]. Linear, quadratic, B/W concentric annuli, and graded index apertures is suggested by Hamed et. al. [14-20]. They computed the PSF considering the above modulated apertures giving lateral resolution improvement. Image analysis of modified Hamming aperture and an application on confocal microscopy and holography is given in [20]. Modulated-alignment dual-axis (MAD) confocal microscopy for deep optical sectioning in tissues is presented in [21]. While an image scanning microscopy with a quadrant detector is recently investigated [22].

Since few studies on the aberration and displacement of objective lenses due to misaligned optics are presented [17], hence this study on the misaligned linear and quadratic apertures applied on the CSLM is made.

It is easy to align the first objective lens of the CSLM, while it is not the case for the second objective. Hence, we assume that the later objective is subjected to tilting and to a lateral shift with respect to the first aligned objective. The PSF in case of misaligned linear and quadratic apertures is computed and compared with the precedent study made by Hamed in [17, 18], in case of misaligned transparent circular apertures. In addition, the CTF in case of aligned and misaligned objectives provided with linear and quadratic apertures is computed. Finally, the contrast of the reconstructed images using the CSLM in different combinations of aligned and misaligned apertures using linear and quadratic apertures is discussed.

THEORETICAL ANALYSIS

In this study, we investigate the PSF in case of misaligned linear and quadratic apertures.

Consider the CSLM under investigation as shown in the figure (1), where the first objective is aligned perfectly and the second objective is

displaced laterally by a radial amount of ρ_d. In this case, we write the complex amplitude as the first aligned aperture of linear distribution as follows:

$$P_1(\rho;\ \alpha) = \rho \exp[jk\,\rho sin(\alpha)]\ ; \qquad |\frac{\rho}{\rho_{01}}| \leq 1 \tag{1}$$

Where j = √-1 , k = 2π/λ , ρ is the radial coordinate in the aperture plane

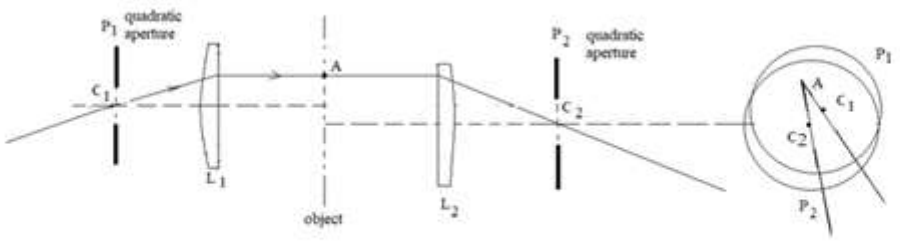

Figur1. *Set- up of misaligned optical system with laterally displaced objectives using quadratic apertures in the CSLM.*

While the complex amplitude for the second displaced linear aperture is written as follows:

$$P_2(\rho;\ \beta, \rho_d) = (\rho - \rho_d)\ \exp[jk\,\rho sin(\beta)]\ ;\ \ |\frac{\rho}{\rho_{02}}| \leq 1 \tag{2}$$

Where α , β are the tilting angles of the corresponding objectives L_1 and L_2.

Similar equations are written, for the quadratic apertures where the first objective is aligned while the second is laterally displaced, as follows:

$$P_3(\rho;\ \alpha) = \rho^2 \exp[jk\,\rho sin(\alpha)]\ ;\ |\frac{\rho}{\rho_{01}}| \leq 1 \tag{3}$$

$$P_4(\rho;\ \beta, \rho_d) = (\rho - \rho_d)^2 \exp[jk\,\rho sin(\beta)]\ ;\ \ |\frac{\rho}{\rho_{02}}| \leq 1 \tag{4}$$

Making use of the Fourier transform operations and convolution product, we are able to get the PSF corresponding to each aperture as follows:

The PSF for the first aligned linear aperture, represented by equation (1), is solved to give the following result:

$$\begin{aligned} h_1(r) = F.T.[\,P_1(\rho;\ \alpha)] &= F.T.\{\,\rho \exp[jk\,\rho sin(\alpha)]\} \\ &= F.T.\{\rho\} \otimes F.T.\{\,\exp[jk\,\rho sin(\alpha)]\} \\ &= F.T.\{\rho\} \otimes \delta(r - f \sin\alpha) \end{aligned} \tag{5}$$

Since $F.T.\{\rho\} = 2\pi\left[\frac{J_1(W)}{W} + \frac{J_0(W)}{W^2} - 2\sum_i \frac{J_i(W)}{W^3}\right];\ ref.[15]$ (6)

From equations 5 and 6, we finally get h_1 for the 1st aligned linear aperture as follows:

$$h_1(W;\alpha) = 2\pi\left[\frac{J_1(W')}{W'} + \frac{J_0(W')}{W'^2} - 2\sum_i \frac{J_i(W')}{W'^3}\right] \tag{7}$$

where $w' = \frac{2\pi\rho_{01}}{\lambda f}(r - f\ sin\alpha)$ is the reduced coordinate in the Fourier plane.

The PSF for the displaced linear aperture represented by equation (2) is solved by operating the F.T. to give the following result:

$$h_2(r) = F.T.\{(\rho - \rho_d)\exp[jk\,\rho sin(\beta)]\}$$

$$= F.T.\{(\rho)\exp[jk\,\rho sin(\beta)]\} - F.T.\{(\rho_d)\exp[jk\,\rho sin(\beta)]\}$$

$$= F.T.[(\rho)] \otimes F.T.\{\exp[jk\,\rho sin(\beta)]\} - (\rho_d) F.T.\{\exp[jk\,\rho sin(\beta)]\}$$

$$= [F.T.(\rho)] \otimes \delta(r - f\sin\beta) - (\rho_d)\delta(r - f\sin\beta)$$

$$= \left\{2\pi\left[\frac{J_1(W)}{W} + \frac{J_0(W)}{W^2} - 2\sum_i \frac{J_i(W)}{W^3}\right]\right\} \otimes \delta(r - f\sin\beta) - (\rho_d)\delta(r - f\sin\beta) \quad (8)$$

We finally, get the following result for the PSF:

$$h_2(W;\beta,\rho_d) = 2\pi\left[\frac{J_1(W'')}{W''} + \frac{J_0(W'')}{W''^2} - 2\sum_i \frac{J_i(W'')}{W''^3}\right] - (\rho_d)\,\delta(r - f\sin\beta) \quad (9)$$

Where $W'' = \frac{2\pi\rho_{02}}{\lambda f}(r - f\,sin\beta)$ *is the reduced coordinate in the Fourier plane.*

Hence, the resultant PSF for the CSLM provided with linear apertures one aligned while the second misaligned is computed from the following equation:

$$h_r(linear\ apert.) = h_1(W;\alpha)\ .h_2(W;\beta,\rho_d) \quad (10)$$

In case of quadratic aperture, the PSF for the first aligned quadratic aperture, represented by equation (3), is solved to give the following result:

$$h_3(r) = F.T.\{\rho^2 \exp[jk\,\rho sin(\alpha)]\}\ ;$$

$$= F.T.\{\rho^2\} \otimes F.T.\{\exp[jk\,\rho sin(\alpha)]\}$$

$$= F.T.\{\rho^2\} \otimes \delta(r - f\sin\alpha) \quad (11)$$

Since $F.T.\{\rho^2\} = 2\pi\left[\frac{J_1(W)}{W} - 2\,\frac{J_2(W)}{W^2}\right];\ ref.[16]$ (12)

From equations 11 and 12, we finally get h_3 for the 1st aligned quadratic aperture as follows:

$$h_3(W;\alpha) = 2\pi\left[\frac{J_1(W')}{W'} - 2\,\frac{J_2(W')}{W'^2}\right] \quad (13)$$

Where W' is defined as for the linear aperture.

While the PSF for the displaced quadratic aperture represented by equation (4) is solved by operating the F.T. to give the following result:

$$h_4(r) = F.T.\{(\rho - \rho_d)^2 \exp[jk\,\rho sin(\beta)]\} \quad (14)$$

$$= F.T.\{(\rho^2 - 2\rho\rho_d + {\rho_d}^2)\exp[jk\,\rho sin(\beta)]\}$$

$$= F.T.\{\rho^2 \exp[jk\,\rho sin(\beta)]\} - 2\rho_d\,F.T.\{\rho\exp[jk\,\rho sin(\beta)]\} + {\rho_d}^2 F.T.\{\exp[jk\,\rho sin(\beta)]\}$$

The 1st term is given for the aligned quadratic aperture represented in equation (12), the 2nd term is given in equation (7) multiplied by a constant value $2\rho_d$, while the 3rd term is simply shifted Dirac-delta function located at $f\,sin\beta$ in the Fourier plane of radial coordinate r and multiplied by the shift squared ${\rho_d}^2$.

Finally, the PSF for the 2nd shifted quadratic aperture is obtained as follows:

$$h_4(W;\beta,\rho_d) = 2\pi\left\{\left[\frac{J_1(W'')}{W''} - 2\,\frac{J_2(W'')}{W''^2}\right] - 2\rho_1\left[\frac{J_1(W'')}{W''} + \frac{J_0(W')}{W''^2} - 2\sum_i \frac{J_i(W'')}{W''^3}\right]\right\}$$

$$+{\rho_d}^2\delta(r - f\sin\beta) \quad (15)$$

Where W'' is defined as in the case of shifted linear aperture.

The RPSF for the CSLM provided with quadratic apertures one aligned while the second misaligned is computed from the following equation:

$$h_r(quadratic\ apert.) = h_3(W;\alpha)\ .h_4(W;\beta,\rho_d) \tag{16}$$

For collimated parallel rays incident upon the apertures, the inclination angles α , β are equal to zero. Hence, the PSF represented by equations 7, 9, 13, and 15 becomes:

$$h_1(W) = 2\pi\left[\frac{J_1(W)}{W} + \frac{J_0(W)}{W^2} - 2\sum_i \frac{J_i(W)}{W^3}\right];\quad 1st\ aligned\ linear\ aperture \tag{17}$$

$$h_2(W;\rho_d) = 2\pi\left[\frac{J_1(W)}{W} + \frac{J_0(W)}{W^2} - 2\sum_i \frac{J_i(W)}{W^3}\right] - (\rho_d)\,\delta(r)\ ;\quad 2nd\ shifted\ linear\ aperture \tag{18}$$

$$h_3(W) = 2\pi\left[\frac{J_1(W)}{W} - 2\,\frac{J_2(W)}{W^2}\right]\ ;1st\ aligned\ quadratic\ aperture \tag{19}$$

$$h_4(W;\rho_d) = 2\pi\left\{\left[\frac{J_1(W)}{W} - 2\,\frac{J_2(W)}{W^2}\right] - 2\rho_d\left[\frac{J_1(W)}{W} + \frac{J_0(W)}{W^2} - 2\sum_i \frac{J_i(W)}{W^3}\right]\right\}$$

$$+\rho_d{}^2\,\delta(r)\ ;2nd\ shifted\ quadratic\ aperture \tag{20}$$

From equations 17, 18 we get the following result for the effective PSF as:

$$h_{eff}(linear\ apert.) = h_1(W).h_2(W;\rho_d)$$

$$= h_1(W)\left[h_1(W) - (\rho_d)\delta(r)\right]$$

$$= h_1{}^2(W) - (\rho_d)\,\delta(r)\,h_1(W) \tag{21}$$

The 1st term is the effective or resultant PSF for perfect alignment of both objectives of linear apertures while the 2nd term $=(\rho_1)\,\delta(r)\,h_1(W)$ is the aberration due to misalignment corresponding to the 2nd objective.

Following similar procedure for the quadratic aperture using equations (19, 20), we get the following result for the effective PSF as:

$$h_4(W;\rho_d) = h_3(W) - 2(\rho_d)\,h_1(W) + \rho_d{}^2\,\delta(r)$$

$$h_{eff}(quadratic\ apert.) = h_3(W).h_4(W;\rho_d)$$

$$= h_3(W)\,[h_3(W) - 2(\rho_d)\,h_1(W) + \rho_d{}^2\,\delta(r)]$$

$$= h_3{}^2(W) - 2(\rho_d)\,h_1(W)\,h_3(W) + \rho_d{}^2\,\delta(r)\,h_3(W) \tag{22}$$

The 1st term in equation (22) represents the effective or resultant PSF for perfect alignment of both objectives of quadratic apertures while the sum of the 2nd and 3rd terms is the aberration due to misalignment of the 2nd objective.

Hence, the misalignment aberration term due to shifted quadratic aperture is given as follows:

$$g(W;\rho_d) = [\rho_d{}^2\,\delta(r) - 2(\rho_d)\,h_1(W)]\,h_3(W) \tag{23}$$

It is clear that for perfectly aligned optical system for the objectives of the CSLM, the misaligned term in equation (23) is disappeared since $\rho_d = 0$ as expected.

Following the analysis made in ref. [18] for circular apertures where the second objective of the CSLM is subjected to tilting and to a lateral shift, we obtain for the misaligned linear and quadratic apertures the following results:

For collimated laser beam, assume that the 2nd objective is subjected to only a lateral shift ρ_d , the radial Bessel integral is written for the linear aperture as follows:

$$h_2(W;\rho_d) = 2\pi\int_{-\rho_{02}+\rho_d}^{\rho_{02}+\rho_d} \rho\ J_0\left(\frac{2\pi\rho r}{\lambda f}\right)\rho\,d\rho \tag{24}$$

Using the properties of Bessel function and integration by parts in, we finally get the following result for shifted objective having linear aperture:

$$h_{2\ linear}\ (W;\ \rho_d) = 4\pi\ (\rho_{02} + \rho_d)^3\ \{\left[\frac{J_1(W_H)}{W_H} + \frac{J_0(W_H)}{{W_H}^2} - 2\sum_i \frac{J_i(W_H)}{{W_H}^3}\right] - (\frac{\varepsilon - 1}{\varepsilon + 1})^3 \left[\frac{J_1(W_L)}{W_L} + \frac{J_0(W_L)}{{W_L}^2} - 2\sum_i \frac{J_i(W_L)}{{W_L}^3}\right]\} \quad (25)$$

For the shifted quadratic aperture, we solve the following radial integral:

$$h_4\left(W\ ;\ \rho_d\right) = 2\pi \int_{-\rho_{02}+\rho_d}^{\rho_{02}+\rho_d} \rho^2\ \ J_0\left(\frac{2\pi\rho\, r}{\lambda f}\right)\rho\, d\rho \quad (26)$$

We finally get the PSF for the shifted objective which has quadratic aperture as follows:

$$h_{4\ quadratic}\ (W;\ \rho_d) = 4\pi\ (\rho_{02} + \rho_d)^4\ \ \{\left[\frac{J_1(W_H)}{W_H} - 2\ \frac{J_2(W_H)}{{W_H}^2}\right] - (\frac{\varepsilon - 1}{\varepsilon + 1})^4 \left[\frac{J_1(W_L)}{W_L} - 2\ \frac{J_2(W_L)}{{W_L}^2}\right]\} \quad (27)$$

The results of PSF for the shifted objective provided with linear and quadratic apertures in equation 25, 27 are compared with the shifted objective corresponding to circular aperture represented by the following equation (28):

$$h_{2\ circular}\ (W;\ \rho_d) = 4\pi\ (\rho_{02} + \rho_d)^2\ \{\left[\frac{J_1(W_H)}{W_H}\right] - (\frac{\varepsilon - 1}{\varepsilon + 1})^2 \left[\frac{J_1(W_L)}{W_L}\right]\} \quad (28)$$

$where\ \varepsilon = \frac{\rho_d}{\rho_{02}} \ll 1$ in all equations (25), (27), and (28).

Where the upper and lower reduced coordinates are written as follows:

$$W_H = \frac{2\pi(\rho_{02} + \rho_d)}{\lambda f}\, r = \frac{2\pi}{\lambda} N.A.\left(1 + \frac{\rho_d}{\rho_{02}}\right) r \quad (29)$$

$$W_L = \frac{2\pi(-\rho_{02} + \rho_d)}{\lambda f}\, r = \frac{2\pi}{\lambda} N.A.\ \left(\frac{\rho_d}{\rho_{02}} - 1\right) r \quad (30)$$

The numerical aperture corresponding to the second objective is, NA = $\frac{\rho_{02}}{f}$ and f is its focal length.

It is known that the CTF for the CSLM is computed from the convolution product corresponding to the apertures of the microscope objectives. It gives maximum value of unity in the center and decreases until reaches zero when the two apertures are completely separated. When the microscope objectives are affected by a displacement in its plane, the maximum value of the CTF is decreased as expected.

An empirical formula for the maximum value of the CTF is given corresponding to one aligned objective with quadratic or linear aperture while the second has the same aperture distribution but displaced by an amount of delta ro. The aperture radius =ro

$$C(\rho) = P_1(\rho) * P_2(\rho) \quad (31)$$

Then, $C_{max}\ (\rho = 0) = 1$; two aligned objectives each has either linear or quadratic aperture.

In case, of one aligned objective of one aligned linear or quadratic aperture and the 2nd objective has misaligned linear or quadratic aperture, the maximum value of the CTF is expressed by the following empirical formula:

$$C_{max}\ (\delta\rho) = \exp[-\alpha\pi\ (\delta\rho/\rho_0)] \quad (32)$$

Where α is a parameter, its value is dependent on the aperture distribution. The maximum value of the CTF becomes unity when the displacement $\delta\rho = 0$.

The contrast of the output images in the CSLM is computed using either of these formulae:

Contrast = I_{max} / I_{min} (33)

Or

Contrast = $1 + [0.5 *(I_{max} - I_{min}) / I\ max]$ (34)

The accurate method to compute the contrast of an image is based on computing the standard deviation (root mean square) of pixel luminance in an image, divided by the average luminance of the whole image. The formula for computation is as follows:

$$Contrast = \left(\frac{1}{N \times M}\right)\frac{sqrt\{\sum_{i=1}^{M}\sum_{j=1}^{N}(L(i,j) - < L >)^2}{< L >} \quad (35)$$

Where the average luminance < L > is calculated as follows:

$$< L > = \left(\frac{1}{N \times M}\right)\sum_{i=1}^{M}\sum_{j=1}^{N} L(i,j) \quad (36)$$

RESULTS AND DISCUSSION

We have considered the PSF of aligned and misaligned circular apertures. In Fig. (2-a) we considered the PSF of aligned circular aperture for the 1st objective. The cut- off spatial frequency is $r_c / \lambda f$ = 818.2 nm/λ f , for NA = 0.5. In Fig. (2-b) we consider the PSF of linear aperture for the 1st objective. The cut- off spatial frequency is $r_c / \lambda f$ = 757.6 nm/λ f , for NA = 0.5.In Fig. (2-c) we considerthe PSF of aligned quadratic aperture for the 1st objective. The cut- off spatial frequency is $r_c / \lambda f$ = 697 nm/λ f , for NA = 0.5. From the three figures we find that quadratic aperture has narrower main lobe than that of linear aperture. Further, the linear aperture has main lobe narrower than that of uniform circular aperture, as expected.In Fig. (3-a) we consider the PSF of a displaced linear aperture for the 2nd objective, where $\frac{\rho_d}{\rho_{02}} = 0.1$. The cut- off spatial frequency is $r_c / \lambda f$ = 757.6 nm/λ f , for NA =0.5.In Fig. (3-b) we consider the PSF

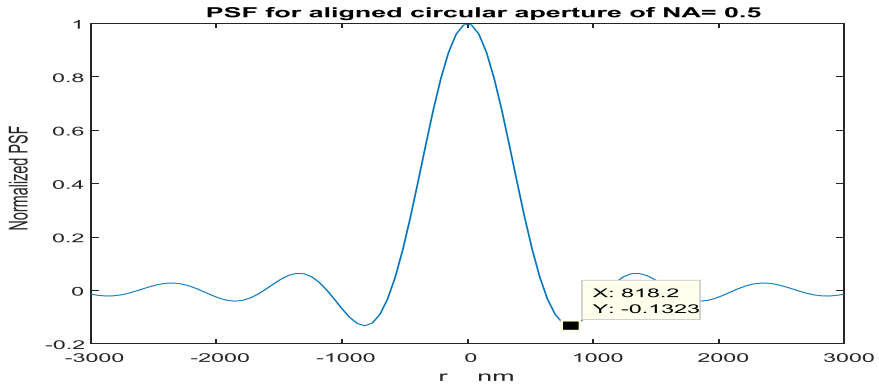

Figure (2- a): *The PSF using aligned circular aperture for the 1st objective. The cut- off spatial frequency is $r_c / \lambda f$ = 818.2 nm/λ f , for NA = 0.5. Two complete side lobes are shown on the graph for $r_{max.}$ = 3000 nm.*

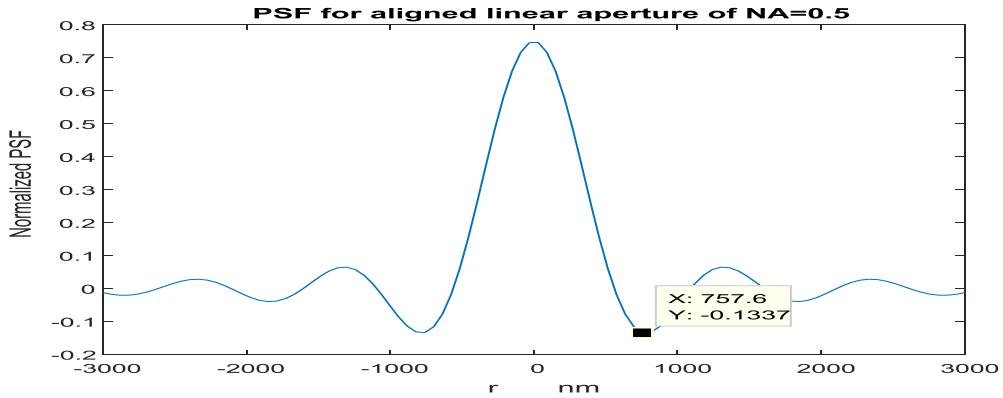

Figure (2- b): *The PSF using aligned linear aperture for the 1st objective. The cut- off spatial frequency is $r_c / \lambda f$ = 757.6 nm/λ f , for NA = 0.5. Two complete side lobes are shown on the graph for $r_{max.}$ = 3000 nm.*

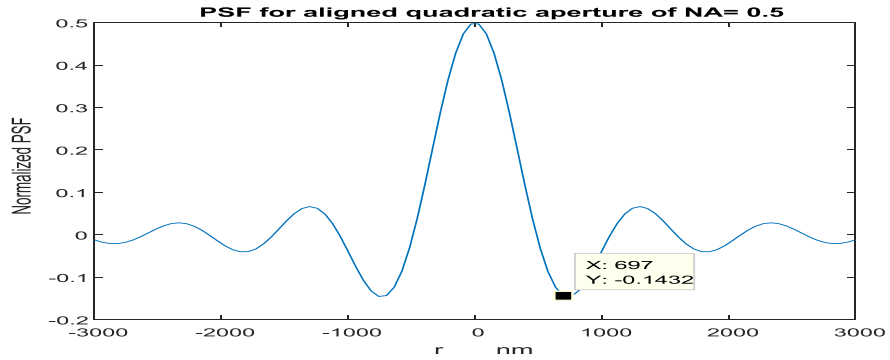

Figure (2- c): *The PSF using aligned quadratic aperture for the 1st objective. The cut- off spatial frequency is r_c /λ f = 697 nm/λ f , for NA = 0.5.*

Two complete side lobes are shown on the graph for r $_{max.}$= 3000 nm. of a displaced quadratic aperture for the 2nd objective, where $\frac{\rho_d}{\rho_{02}} = 0.1$.The cut- off spatial frequency is r_c / λ f = 575.8 nm// λ f , for NA = 0.5.From these two figures we can find that the quadratic aperture has a PSF that is narrower than that of linear aperture, as compared with the similar results for the aligned apertures.

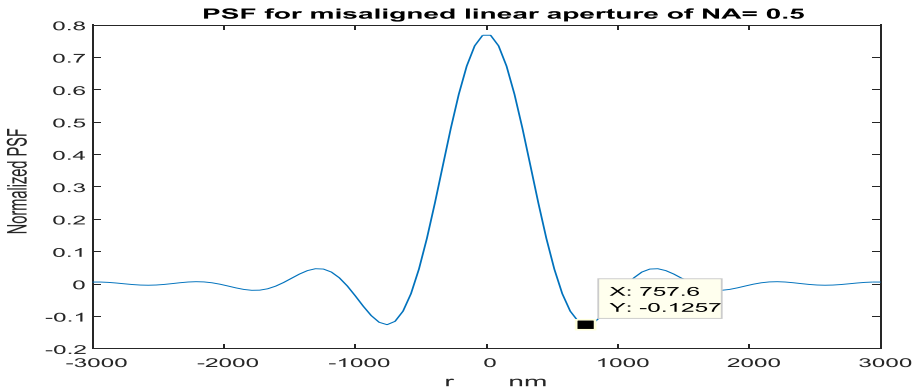

Figure (3- a): *The PSF using displaced linear aperture for the 2nd objective, where $\frac{\rho_d}{\rho_{02}} = 0.1$. The cut- off spatial frequency is r_c/ λ f = 757.6 nm/λ f , for NA = 0.5.*

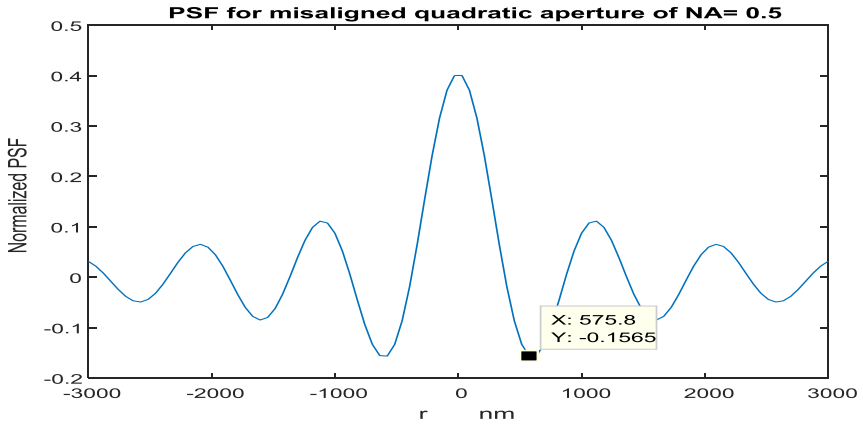

Figure (3- b): The PSF using displaced quadratic aperture for the 2nd objective, where $\frac{\rho_d}{\rho_{02}} = 0.1$.The cut- off spatial frequency is r_c/ λ f = 575.8 nm/λ f , for NA = 0.5.

In Fig. (4-a) we consider the effective PSF of only using displaced linear aperture for the 2nd objective, where $\frac{\rho_d}{\rho_{02}} = 0.1$.The cut- off spatial frequency is r_c / λ f = 515.2 nm/λ f , for NA = 0.5. In Fig. (4-b) we consider The effective PSF using only displaced quadratic aperture for the 2nd objective, where $\frac{\rho_d}{\rho_{02}} =$ 0.1.The cut- off spatial frequency is r_c / λ f = 393.9 nm/λ f , for NA = 0.5. Again for the misaligned case we have effective PSF narrower for the quadratic case than that for the linear aperture.

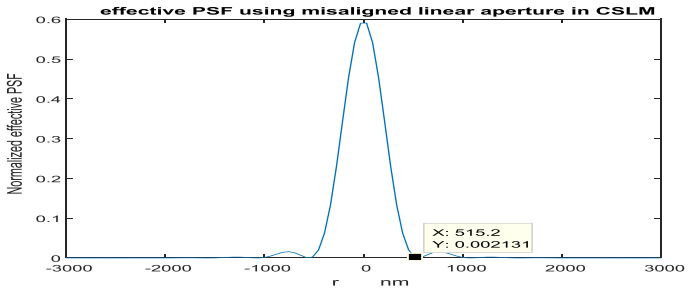

Figure (4- a): *The effective or resultant PSF using displaced linear aperture for the 2ndobjective, where* $\frac{\rho_d}{\rho_{02}} = 0.1$.*The cut- off spatial frequency is rc / λ f = 515.2 nm/λ f , for NA = 0.5.*

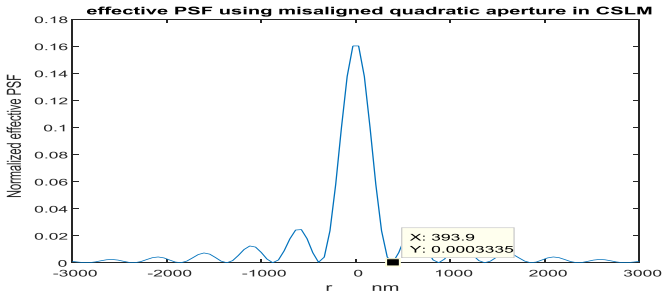

Figure (4- b): *The effective or resultant PSF using displaced quadratic aperture for the 2nd objective, where* $\frac{\rho_d}{\rho_{02}} = 0.1$.*The cut- off spatial frequency is* $r_c / \lambda f = 393.9$ *nm/λ f , for NA = 0.5.*

In addition, we have only one side lobe in the effective PSF using displaced linear aperture for the 2nd objective as shown in the figure (4- a), while many lobes are shown in case of displaced quadratic aperture as shown in the figure (4- b).In Fig. (5-a) we consider the image of a point using two misaligned linear apertures in the CSLM where NA = 0.5. The cut- off spatial frequency is $r_c / \lambda f = 393.9$ nm/λ f . In Fig. (5- b) we consider the image of a point using two misaligned quadratic apertures in the CSLM where NA = 0.5. The cut- off spatial frequency is $r_c / \lambda f = 333.3$ nm/λ f. In both figures we have only one side lobe and the other is highly suppressed. Again, in the quadratic case we get a curve that narrower than that of the linear one.

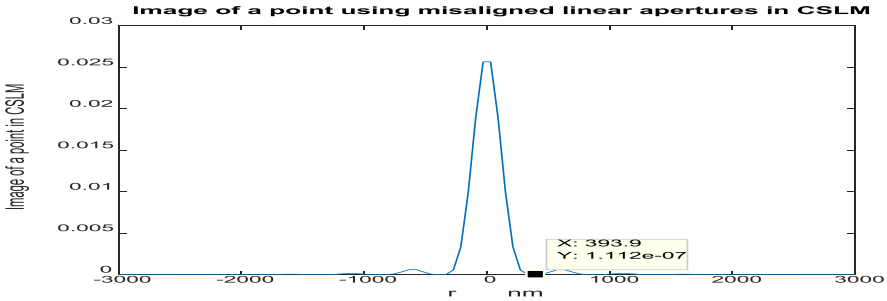

Figure (5- a): *The plot represents the image of a point using two misaligned linear apertures in the CSLM where NA = 0.5. The cut- off spatial frequency is* $r_c / \lambda f = 393.9$ *nm/λ f .*

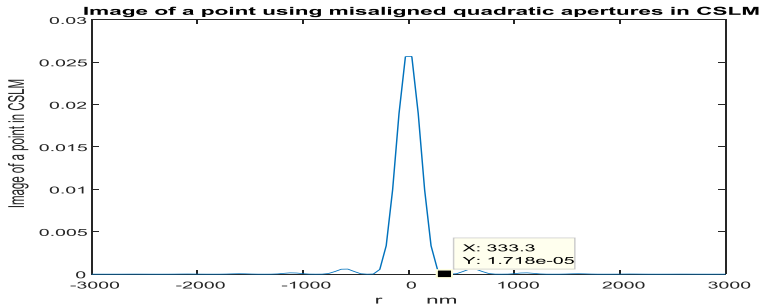

Figure (5- b): *The plot represents the image of a point using two misaligned quadratic apertures in the CSLM where NA = 0.5. The cut- off spatial frequency is* $r_c / \lambda f = 333.3$ *nm/λ f . One side loop is shown while the others are truncated.*

In Fig. (6-a) we consider the effective PSF of using aligned linear aperture for the 1st objective, while the 2nd objective with quadratic aperture is displaced by ρ_d, where $\frac{\rho_d}{\rho_{02}} = 0.1$.The cut- off spatial frequency is $r_c / \lambda f$ = 454.5 nm/λ f , for NA = 0.5 for both apertures. From the figure we find highly attenuated side lobes. In Fig. (6-b) we consider the image of a point using aligned linear aperture for the 1st objective, while the 2nd objective with quadratic aperture is displaced by ρ_d, where $\frac{\rho_d}{\rho_{02}} = 0.1$.The cut- off spatial frequency is $r_c / \lambda f$ = 333.3 nm/λ f , for NA = 0.5 for both apertures. It is clear from the figure that side lobes are totally suppressed.

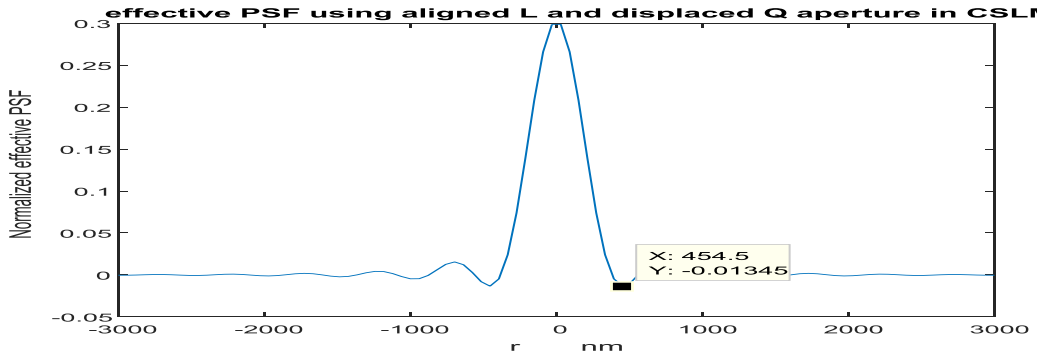

Figure (6- a): *The effective or resultant PSF using aligned linear aperture for the 1st objective, while the 2nd objective with quadratic aperture is displaced by ρ_d, where $\frac{\rho_d}{\rho_{02}} = 0.1$.*

The cut- off spatial frequency is $r_c / \lambda f$ = 454.5 nm/λ f , for NA = 0.5 for both apertures. It is shown that, the side loops are attenuated.

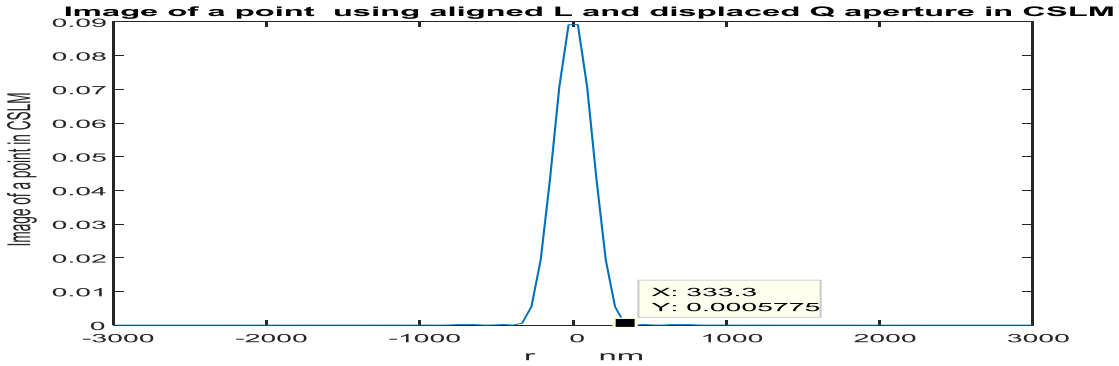

Figure (6- b): *The image of a point using aligned linear aperture for the 1st objective, while the 2nd objective with quadratic aperture is displaced by ρ_d, where $\frac{\rho_d}{\rho_{02}} = 0.1$.*

The cut- off spatial frequency is $r_c / \lambda f$ = 333.3 nm/λ f , for NA = 0.5 for both apertures. It is shown that, the side loops are disappeared or truncated.

In Fig. (7-a) we consider the PSF of aligned quadratic aperture for the 1st objective. The cut-off spatial frequency is $r_c / \lambda f$ = 939.4 nm/λ f. NA = 0.4. In Fig. (7-b) we consider the PSF of misaligned quadratic aperture for the 2nd objective, subjected to a lateral shift where $\frac{\rho_d}{\rho_{02}} = 0.1$ and NA = 0.4. The cut- off spatial frequency is $r_c / \lambda f$ = 757.6 nm/λ f. We can see from these two figures that the PSF in the misaligned case is narrower than that of the aligned. In Fig. (7-c) we have the PSF of aligned quadratic aperture with NA=0.4 we have the 1st secondary peak located at 1606 nm. In Fig. (7-d) we have the PSF of misaligned quadratic aperture with NA=0.4. From the figure we can see that the 1st secondary peak located at 1364 nm. 10% lateral shift w.r.t the maximum radius of the quadratic aperture is assumed.

The central peak has nearly 0.8 as compared with unity for the aligned quadratic aperture. In Fig. (7-e) we consider the PSF aligned and misaligned quadratic aperture. In this figure we can find that the 1st secondary peaks in the PSF of the 1st aligned objective and the 2nd displaced objective located at 1727, 1364 nm respectively. The displacement corresponding to the 2nd objective has 0.1 the aperture radius.

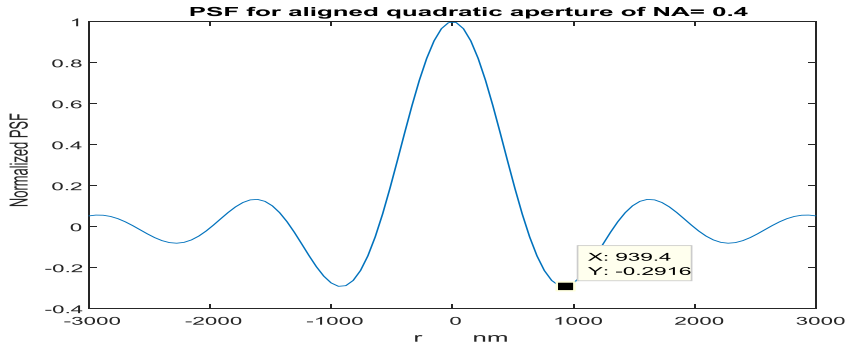

Figure (7- a): *The PSF using aligned quadratic aperture for the 1st objective. The cut- off spatial frequency is $r_c / \lambda f$ = 939.4 nm/λ f. NA = 0.4. One and nearly half side lobes are shown on the graph for $r_{max.}$ = 3000 nm.*

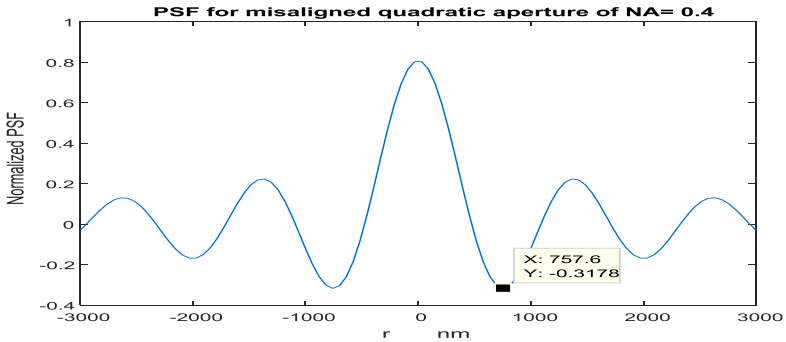

Figure (7- b): *The PSF using misaligned quadratic aperture for the 2nd objective, subjected to a lateral shift where* $\frac{\rho_d}{\rho_{02}} = 0.1$ *and NA = 0.4. The cut- off spatial frequency is $r_c/\lambda f$ =757.6 nm/λ f. Two complete side lobes are shown on the graph for $r_{max.}$ = 3000 nm.*

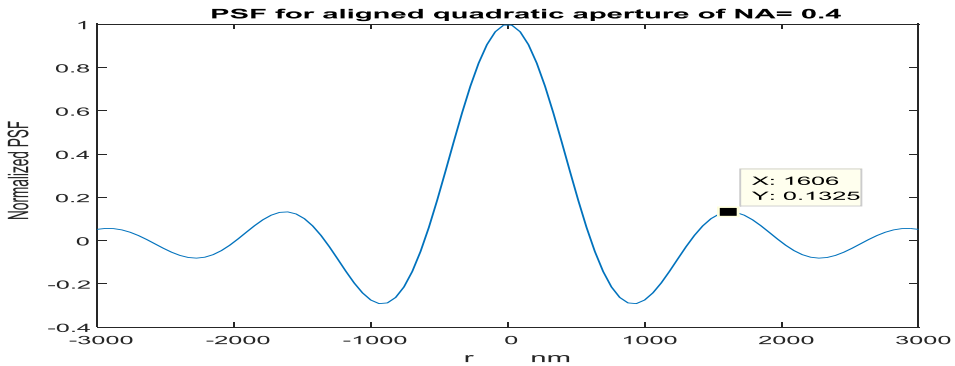

Figure (7- c): *The 1st secondary peak located at 1606 nm.*

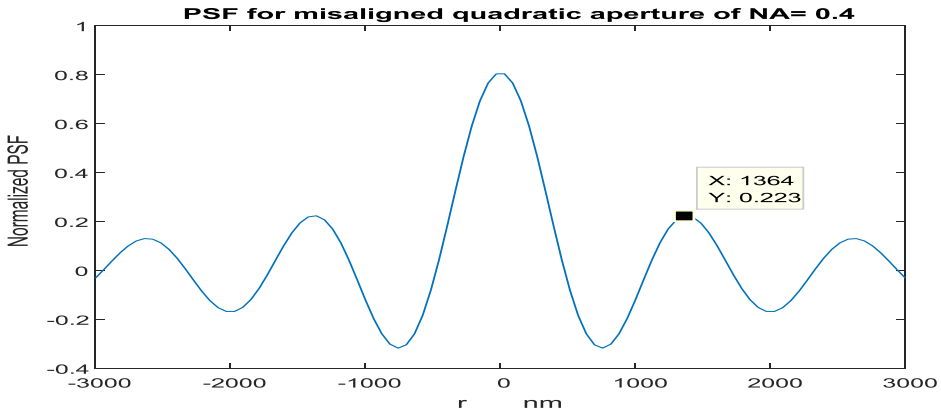

Figure (7- d): *The 1st secondary peak located at 1364 nm. 10% lateral shift w.r.t the maximum radius of the quadratic aperture is assumed. The central peak has nearly 0.8 as compared with unity for the aligned quadratic aperture.*

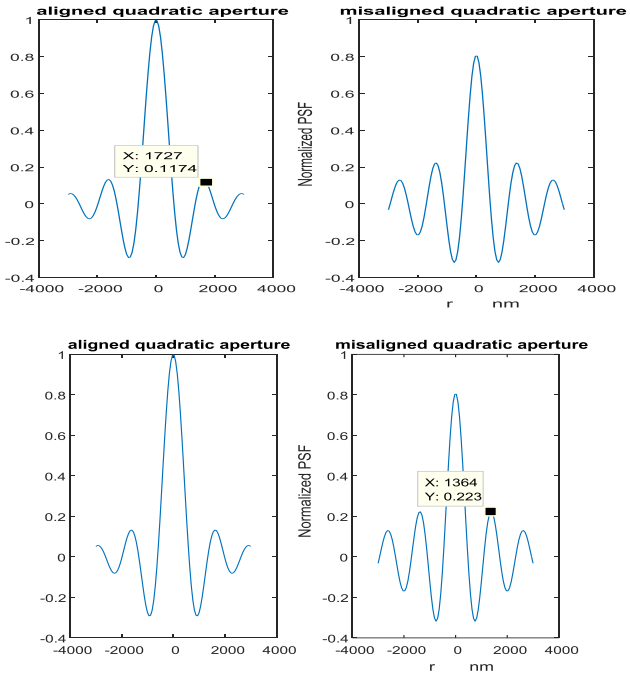

Figure (7- e): *The 1st secondary peaks in the PSF of the 1st aligned objective and the 2nd displaced objective located at 1727, 1364 nm respectively. The displacement corresponding to the 2nd objective has 0.1 the aperture radius.*

In Fig. (8-a) we consider the effective PSF of two aligned quadratic apertures for the objectives of the CSLM. The cut- off spatial frequency is reduced to r_c / λ f = 636.4 nm/λ f. In Fig. (8-b) we consider the effective PSF of two misaligned quadratic apertures for the objectives of the CSLM. Both of the microscope objectives are subjected to a lateral shift where $\frac{\rho_d}{\rho_{02}} = 0.1$. The cut- off spatial frequency is r_c / λ f = 454.5 nm/λ f with NA = 0.4. From these two figure we can find that: first, the central lobe in the misaligned case is narrower than that of the aligned case. Second, the side lobes in the aligned case die out faster than that of the misaligned case.

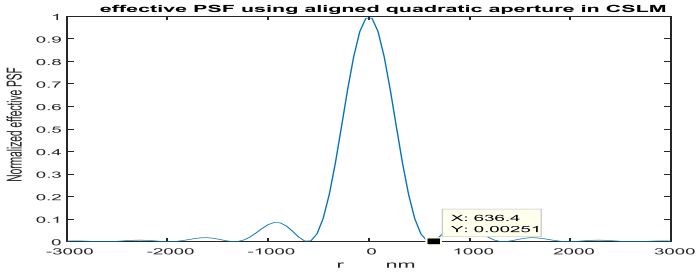

Figure (8- a): *The RPSF using two aligned quadratic apertures for the objectives of the CSLM. The cut- off spatial frequency is reduced to $r_c / \lambda f$ = 636.4 nm// λf.*

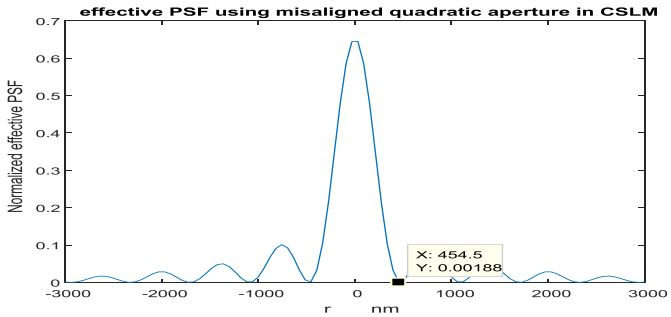

Figure (8- b): *The effective or RPSF using two misaligned quadratic apertures for the objectives of the CSLM. Both of the microscope objectives are subjected to a lateral shift where* $\frac{\rho_d}{\rho_{02}} = 0.1$. *The cut- off spatial frequency is* $r_c / \lambda f$ = 454.5 nm// λf *becomes maximum , at NA = 0.4.*

In Fig. (9-a) we consider the image of a point using two aligned quadratic apertures in the CSLM where NA = 0.4. The cut- off spatial frequency is $r_c / \lambda f$ = 575.8 nm/λ f. In Fig. (9-b) we consider the image of a point using two misaligned quadratic apertures in the CSLM where NA = 0.4. The cut- off spatial frequency is $r_c / \lambda f$ = 454.5 nm/λ f. The lateral shift is $ro_d = 0.1\,\rho_0$ for both of the objectives. From these two figures we find that the image for misaligned case has a narrower central lobe than that of the aligned case. On the other side, side lobes have a smaller level in the aligned case than that of the misaligned case.

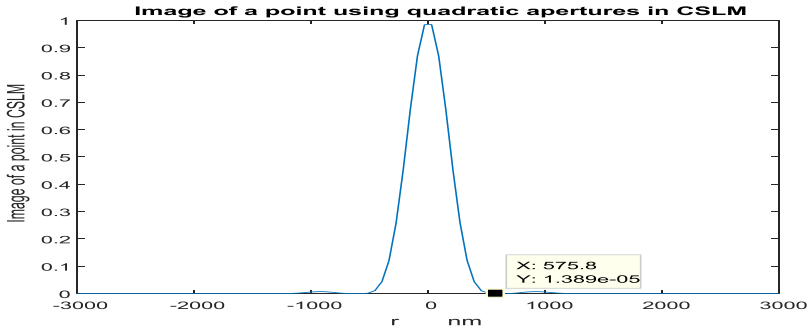

Figure (9- a): *The plot represents the image of a point using two aligned quadratic apertures in the CSLM where NA = 0.4. The cut- off spatial frequency is* $r_c / \lambda f$ *= 575.8 nm// λf .*

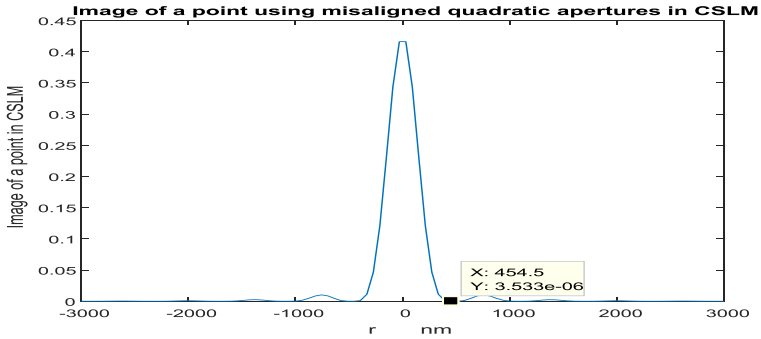

Figure (9- b): *The plot represents the image of a point using two misaligned quadratic apertures in the CSLM where NA = 0.4. The cut- off spatial frequency isr* $_c / \lambda f$ *= 454.5 nm. The lateral shift is* $ro_d = 0.1\,\rho_0$ *for both of the objectives.*

Table1. *The normalized maximum value of the CTF (*C_{max}*), for the modulated quadratic apertures in the CSLM. The 1st objective is aligned while the 2nd objective is displaced by an amount =* δro.

C max	Displacement (δr) in pixels
1.0	0
1.0	1
0.9925	2
0.9852	3
0.9778	4
0.9725	5
0.9343	10
0.899	15
0.8662	20
0.8338	25
0.8024	30
0.7721	35
0.7428	40
0.7127	45
0.6872	50
0.6608	55
0.6355	60
0.6109	65
0.5876	70
0.5649	75

In Fig. (10-a) we consider Bone marrow image of dimensions 1024× 1024 pixels used in the processing**.** In Fig.(10-b) we consider linear apertures in image of 1024× 1024 pixels and radius = 256 pixels. One is centered at (512, 512) pixels, while the other is shifted vertically by a displacement of = 25 pixels. In Fig. (10-c) we consider the Coherent Transfer Function (CTF) computed from direct convolution and FFT technique for the CSLM, where CTF = $P_1 \otimes P_2$ and P_1 and P_2 for linearly distributed apertures. For FFT calculation peak occurs at 513 pixels. In Fig. (10-d) we consider the CTF computed from direct convolution and FFT technique for the CSLM, where P_1 has aligned linear distribution whileP_2 has misaligned linear distribution with displacement = 25 pixels. For FFT calculation peak occurs at 513 pixels. In Fig. (10-e) we consider the output image from the bone marrow image using the CSLM provided with aligned linear apertures for both of the microscope objectives. In the Fig. (10-f) we consider the output image from the bone marrow image using the CSLM provided with one aligned linear aperture and the 2nd has the same linear distribution like the 1st but it is displaced vertically by an amount 25 pixels. In Fig. (10-g) we consider the output image from the bone marrow image using the CSLM provided with two misaligned linear apertures for the microscope objectives. The displacement 25 pixels along y- coordinate is assumed in all plots. In Fig. (11-a) we consider two quadratic apertures and radius = 256 pixels in images of1024× 1024 pixels. One aperture is centered at (512, 512) pixels, while that the other is shifted vertically by a displacement of = 25 pixels. In Fig. (11-b) we consider the CTF computed from direct convolution and FFT technique for the CSLM, where both of P_1 and P_2 have quadratic distributed apertures. For

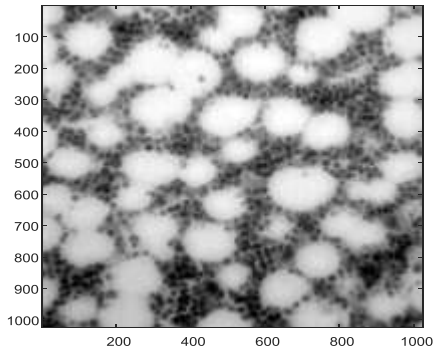

FT calculation peak occurs at 513.

Figure (10- a): *Bone marrow image of dimensions 1024× 1024 pixels used in the processing.*

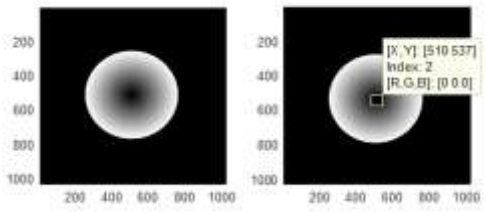

Figure (10- b): *Two images of linear apertures of dimensions 1024× 1024 pixels, and radius = 256 pixels. The image in the left, is centered at (512, 512) pixels, while that shown in the right is shifted vertically by a displacement of d = 537-512 = 25 pixels.*

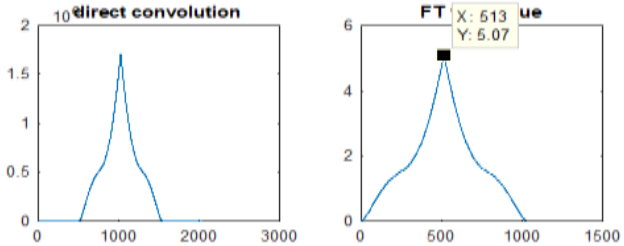

Figure (10- c): *The Coherent Transfer Function (CTF) computed from direct convolution and FFT technique for the CSLM, where CTF = $P_1 \otimes P_2$ and P_1 and P_2 have linearly distributed apertures.*

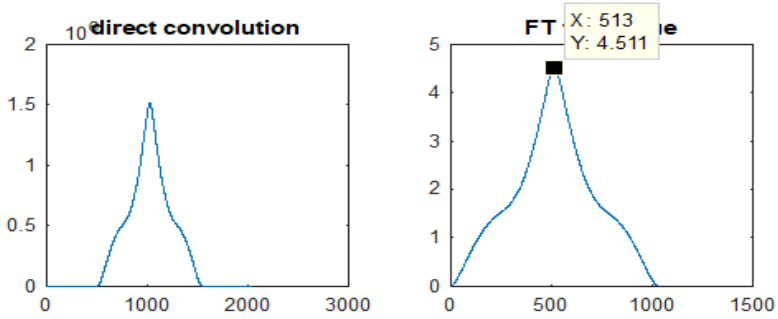

Figure (10- d): *The Coherent Transfer Function (CTF) computed from direct convolution and FFT technique for the CSLM, where CTF = $P_1 \otimes P_2$ and P_1 has aligned linear distribution whileP_2 has misaligned linear distribution with displacement = 25 pixels.*

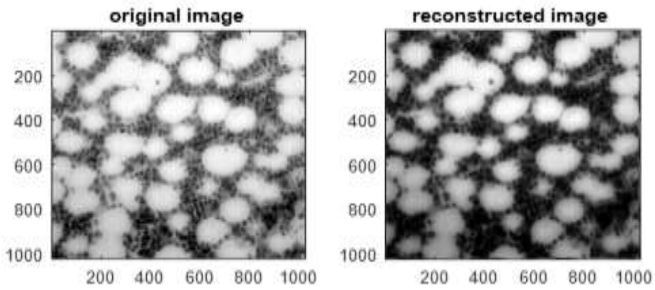

Figure (10- e): *The reconstructed image from the bone marrow image using the CSLM provided with aligned linear apertures for both of the microscope objectives.*

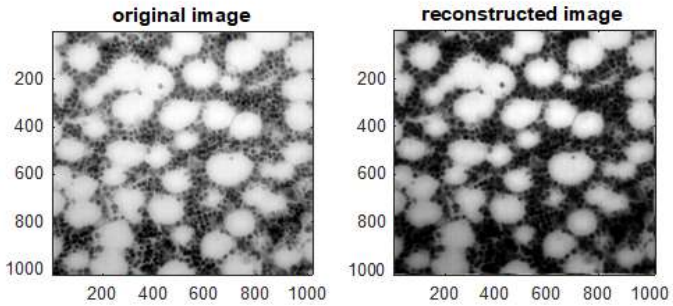

Figure (10- f): *The reconstructed image from the bone marrow image using the CSLM provided with one aligned linear aperture and the 2nd has the same linear distribution like the 1st but it is displaced vertically by an amount 25 pixels.*

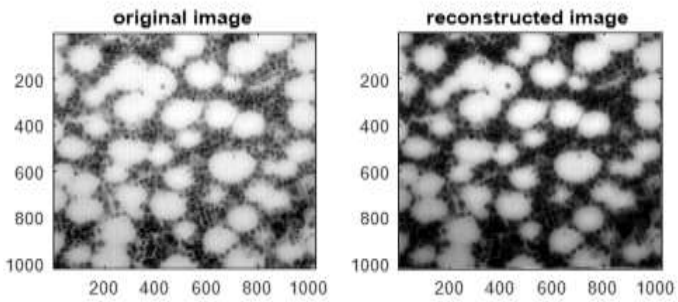

Figure (10- g): *The reconstructed image from the bone marrow image using the CSLM provided with two misaligned linear apertures for the microscope objectives. The displacement is 25 pixels along y- coordinate as shown in the aperture in figure (10- b).*

In Fig. (11-c) we consider the CTF computed from direct convolution and FFT technique for the CSLM, where P_1 has aligned quadratic distribution while P_2 has misaligned quadratic distribution with displacement = 25 pixels. For FFT calculation peak occurs at 514. In Fig. (11-d) we consider the reconstructed image from the bone marrow image using the CSLM provided

with aligned quadratic apertures for the microscope objectives. In Fig. (11-e) we consider the reconstructed image from the bone marrow image using the CSLM provided with one aligned quadratic aperture and the 2nd has the same quadratic distribution like the 1st but it is displaced vertically by an amount = 25 pixels.

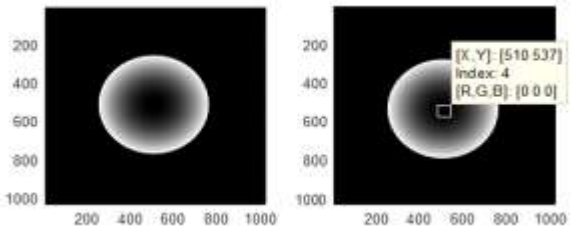

Figure (11- a): *Two images of quadratic apertures of dimensions 1024× 1024 pixels, and radius = 256 pixels. The image in the left, is centered at (512, 512) pixels, while that shown in the right is shifted vertically by a displacement of d = 537-512 = 25 pixels.*

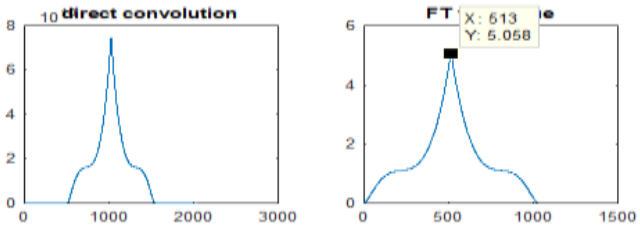

Figure (11- b): *The Coherent Transfer Function (CTF) computed from direct convolution and FFT technique for the CSLM, where CTF = $P_1 \otimes P_2$ and both of P_1 and P_2 have quadratic distributed apertures.*

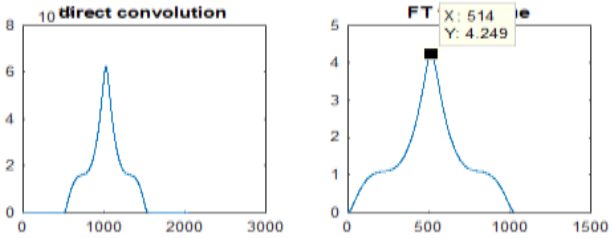

Figure (11- c): *The Coherent Transfer Function (CTF) computed from direct convolution and FFT technique for the CSLM, where CTF = $P_1 \otimes P_2$ and P_1 has aligned quadratic distribution while P_2 has misaligned quadratic distribution with displacement, δ= 25 pixels.*

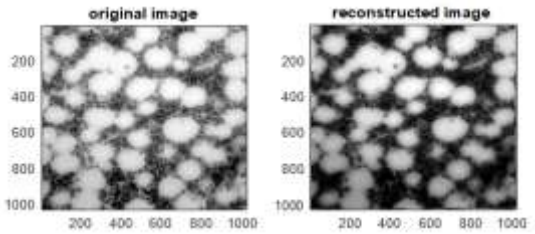

Figure (11- d): *The reconstructed image from the bone marrow image using the CSLM provided with aligned quadratic apertures for the microscope objectives.*

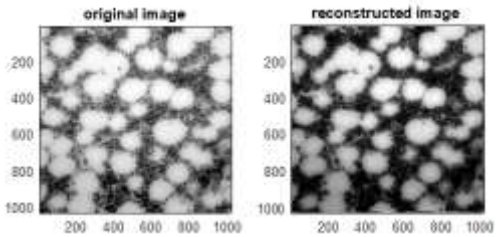

Figure (11- e): *The reconstructed image from the bone marrow image using the CSLM provided with one aligned quadratic aperture and the 2nd has the same quadratic distribution like the 1st but it is displaced vertically by an amount d = 25 pixels.*

we consider normalized plot of the CTF using FFT technique in all the plots shown in the figures (12 a- d). Forboth of P_1 and P_2 have uniform circular apertures, the maximum value of CTF C_{max} = 1.0, as in the figure (12- a). In Fig. (12-b), For both of P_1 and P_2 have quadratic distributed apertures, C_{max} = 1.0. In Fig. (12-c), where both of P_1 and P_2 have quadratic distributed apertures, While the 2nd objective is displaced by ro = 25 pixels, C_{max} = 0.8338. Peak occurs at 514 pixels. In Fig. (12-d), where both of P_1 and P_2 have quadratic distributed apertures, While the 2nd objective is displaced by ro = 50 pixels, C_{max} = 0.6872. The peak occurs at 513 pixels.

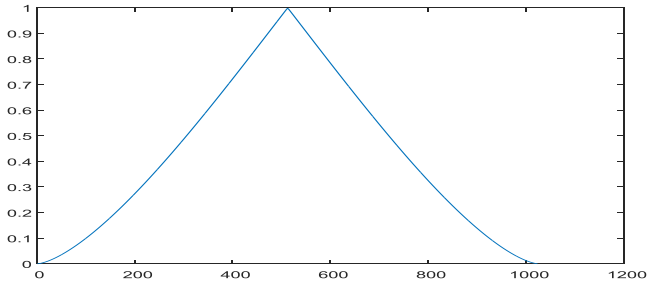

Figure (12- a): *Normalized plot of the CTF using FFT technique, where CTF = $P_1 \otimes P_2$ and both of P_1 and P_2 have uniform circular apertures.*

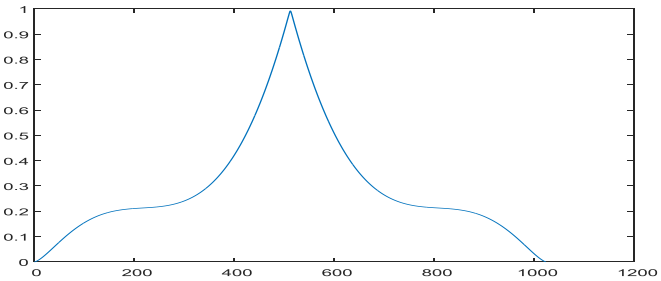

Figure (12- b): *Normalized plot of the CTF using FFT technique, where CTF = $P_1 \otimes P_2$ and both of P_1 and P_2 have quadratic distributed apertures. C_{max} = 1.0.*

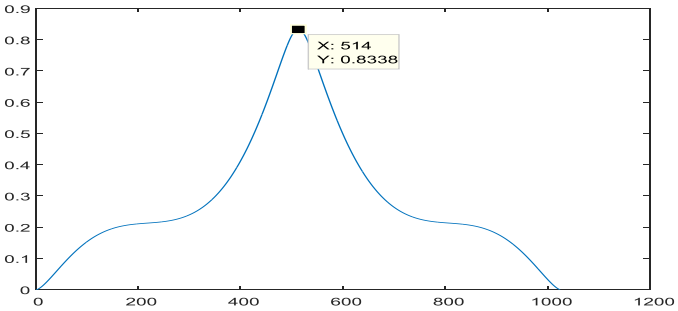

Figure (12- c): *Normalized plot of the CTF using FFT technique, where CTF = $P_1 \otimes P_2$ and both of P_1 and P_2 have quadratic distributed apertures. While the 2nd objective is displaced by ro = 25 pixels. C_{max} = 0.8338.*

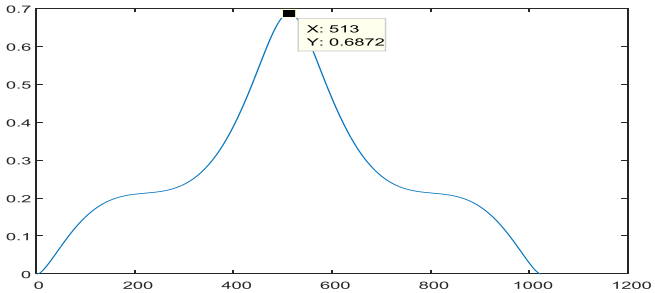

Figure (12- d): *Normalized plot of the CTF using FFT technique, where CTF = $P_1 \otimes P_2$ and both of P_1 and P_2 have quadratic distributed apertures. While the 2nd objective is displaced by ro = 50 pixels. C_{max} = 0.6872.*

In Fig. 13 we consider the normalized plot of the maximum value of the CTF as a function of the displacement (δro) in pixels occurred in the 2nd objective where the 1st objective is assumed aligned. The apertures have quadratic distributions each of radius = 256 pixels. The continuous curve is the maximum CTF computed from the FFT techniques while the discontinuous curve is computed from the empirical formula where is set equal toα = 0.7. It is shown that the computed values from FFT and that computed from empirical formula are in good agreement for small displacement.

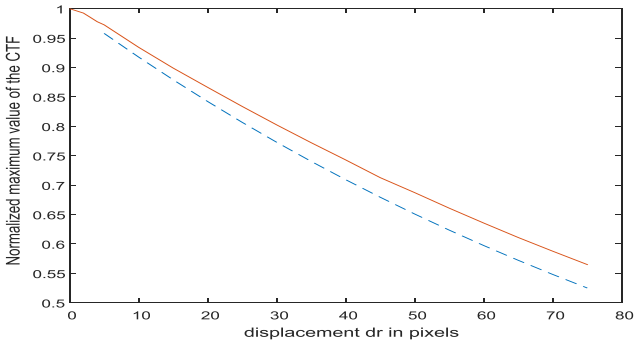

Figure (13): *The Normalized plot of the maximum value of the CTF as a function of the displacement (δro) in pixels occurred in the 2nd objective where the 1st objective is aligned.*

The apertures have quadratic distributions each of radius = 256 pixels. The continuous curve is the maximum CTF computed from the FFT techniques while the discontinuous curve is computed from the empirical formula where α = 0.7.

Table2. *The contrast computed by two methods for the output images versus displacement given to the 2nd objective lens considering modulated quadratic apertures in the CSLM. While the 1st objective is assumed aligned.*

Contrast = I_{max} / I_{min}	Contrast = 1+ 0.5*(I_{max}- I_{min}) /I_{max}	Displacement (δro) in pixels
0.9610	0.9797	0
0.9416	0.9690	2
0.9310	0.9630	3
0.9204	0.9568	4
0.9089	0.9499	5
0.8442	0.9077	10
0.7815	0.8602	15
0.7248	0.8102	20
0.6719	0.7558	25
0.6223	0.6965	30
0.5762	0.6323	35
0.5334	0.5626	40
0.4937	0.4872	45
0.4568	0.4054	50
0.4226	0.3167	55
0.3909	0.2208	60

Table. *The mean value <I>, the standard deviation σ, and the contrast of the reconstructed images versus displacement given to the 2nd objective lens considering modulated quadratic apertures in the CSLM. While the 1st objective is assumed aligned.*

< I >	σ = STD	Image contrast = σ / < I >	Displacement (δro) in pixels
0.4312	0.2703	0.6267	0
0.4027	0.2570	0.6383	5
0.3746	0.2406	0.6423	10
0.3477	0.2239	0.6438	15
0.3225	0.2079	0.6445	20
0.2990	0.1928	0.6450	25
0.2770	0.1787	0.6453	30
0.2565	0.1656	0.6455	35
0.2374	0.1533	0.6457	40

0.2197	0.1419	0.6458	45
0.2033	0.1313	0.6459	50
0.1880	0.1215	0.6460	55
0.1739	0.1123	0.6461	60

Contrast of the original input image = 0.3908 computed from equations (34, 35).

Mean value = 157.74 /256 = 0.6162

Standard deviation = 61.64 /256 = 0.2408

The results of the image contrast, computed from equation (33) for the reconstructed images in the CSLM, versus objective displacement is shown in the table (2). Where the two microscope objectives are provided with quadratic apertures with the 1st objective aligned while the 2nd is displaced by an amount .It is shown that the contrast computed from I_{max} / I_{min} is decreased with aperture displacement as expected. The contrast of the output images is changed from nearly 96 % for two aligned apertures of the microscope objectives to about 39% for displacement = 60 pixels. In addition, the contrast is sensitive to small displacement it decreases from 96% to 90% for nearly 5 pixels.

The accurate formula used to obtain image contrast is computed from equation (34). The results of the mean value $< I >$, the standard deviation σ, and the contrast of the output images versus displacement given to the 2nd objective lens considering modulated quadratic apertures in the CSLM. While the 1st objective is assumed aligned are shown in the table (3). It is shown that the contrast of the output images is much improved as compared with the contrast of the input bone marrow image. While it remains nearly constant at about 0.64 for different displacements changed up to nearly 10% with respect to the aperture radius.

CONCLUSION

We considered aligned and misaligned quadratic apertures. For the case of one misaligned aperture, we have narrower PSF than that for the case of aligned one. Cut-off spatial frequency and position of first peak comes nearer to the main lobe than that of the aligned case. Then we considered the effective PSF for two aligned apertures and two misaligned apertures. Again, in misaligned case the spatial cut-off frequency is lower than that of the aligned case. Moreover, side lobes die faster in the aligned case than that of the misaligned case. Moreover, we considered linear apertures and we found that the PSF has central lobe in the quadratic case narrower than that for the linear. The empirical formula for the maximum CTF outlined in the theoretical analysis is compared with the corresponding CTF computed from the FFT technique as shown in the plot. Consequently, the degree of misalignment is related to the displacement of the 2nd objective for the quadratic aperture. The method is sensitive to displacement of 2 pixels. It is shown that the image contrast is greatly affected by the objective displacement since it changes from 96% to nearly 39% for 10% misalignment. Consequently, the optical confocal system of the microscope is checked for alignment by measuring the image contrast corresponding to the output images computed from I_{max} / I_{min}.

While the computation of the image contrast from the accurate method of STD showed nearly constant values. While the root mean square values are decreased with the displacement. In addition, the mean values are also decreased with the displacement given to either the aperture or the microscope objective. Hence, this method to check alignment of the optical system of the CSLM is evident by measuring either the mean or the root mean square values separately.

REFERENCES

[1] Sheppard C.J.R. The use of lenses with annular aperture in scanning optical microscopy Optik 1977; 48: 329- 334.

[2] Sheppard C.J.R, Choudhury A. Image formation in the scanning microscope.J. Mod. Opt. 1977; 24 (10): 1051- 1073.

[3] Sheppard C.J.R, Wilson T. Depth of field in the scanning microscope.Opt. Letters 1978; 3: 115- 117.

[4] Sheppard C.J.R, Wilson T. Appl. Opt. 1979; 18 (22): 3764- 3769, Imaging properties of annular lenses.

[5] Sheppard C.J.R, Wilson T.Fourier imaging of phase information in conventional and scanning microscopes.Phil. Trans. Roy. Soc. 1980; A295 (14): 513- 536.

[6] Cox I.J, Sheppard C.J.R, Wilson T. Improvement in resolution by nearly confocal microscopy.Appl. Opt.1982; 21: 778- 781.

[7] Sheppard C.J.R, Mao X.Q. Confocal microscopes with slit apertures. J. Mod. Opt. 1988; 35:1169- 1185.

[8] Sheppard C.J.R. Super-resolution in confocal imaging. Optik 1988; 80 (2): 53- 54.

[9] Sheppard C.J.R and Gu M. Improvement of axial resolution in confocal microscopy using annular pupil. Opt. Communication 1991; 84: 7-13.

[10] Gu M, Sheppard C.J.R, Zhou H. Optimization of axial resolution in confocal imaging using annular pupils.Optik 1993; 93 (2): 87- 90.

[11] Cox G and Sheppard C.J.R. Practical limits of resolution in confocal and nonlinear microscopy. Microscopy research and technique 2004; 63 (1): 18- 22.

[12] Sheppard C.J.R, Wilson T. Gaussian beam theory of lenses with annular aperture. IEE J. Microwaves, Optics and Acoustics 1978; 2: 105- 112.

[13] Sheppard C.J.R, Larkin KG.Effect of numerical aperture on interference fringe spacing.Appl. Opt. 1995; 34(22): 4731- 4734.

[14] Clair J.J, Hamed A.M.Theoretical studies on optical coherent microscopes. Optik 1983; 64 (2): 133-141.

[15] Hamed A.M, Clair J.J.Image and super-resolution in optical coherent microscopes. Optik 1983; 64 (4): 277-284.

[16] Hamed A.M, Clair J.J. Studies on optical properties of confocal scanning optical microscope using pupils with radially transmission ρ^n istribution. Optik 983; 65 (3): 209-218.

[17] Hamed A.M. Aberration studies utilizing an optoelectronic coherent microscope. Optik 1984; 67 (3): 279- 290.

[18] Hamed A.M.Excentration errors combined with wave front aberration in a Coherent Scanning Microscope. Optik 1989; 82 (1): 1- 4.

[19] Hamed A.M. A study on amplitude modulation and an application on confocal imaging. Optik 1998; 107 (4): 161- 164.

[20] Hamed A.M, Al-Saeed T. Image analysis of modified Hamming aperture: Application on confocal microscopy and holography. Journal of Modern Optics 2015; 62 (10):801 – 810.

[21] Leigh S.Y. Modulated-alignment dual-axis (MAD) confocal microscopy for deep optical sectioning in tissues. Biomedical Opt. Express 2014; 5 (6): 1709-1720.

[22] Castello M, Sheppard C.J.R, Diaspro A, Vicidomini V. Image scanning microscopy with a quadrant detector. Optics letters 2015; 40 (22): 5355- 5358.

Citation: *A.M. Hamed, Tarek A. Al- Saeed. "A Study on Misaligned Modulated Apertures in Confocal Scanning Laser Microscope (CSLM)", International Journal of Emerging Engineering Research and Technology, 7(3), 2019, pp.9-27*